

DE LA RECHERCHE À L'INDUSTRIE

cea



ESNT

Espace de Structure Nucléaire Théorique

DSM-DAM

www.cea.fr

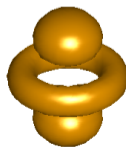
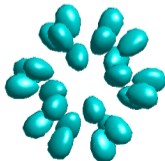
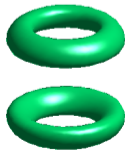
MAGNETIC DIPOLE MOMENTS AS A SIGNATURE OF α -CLUSTERING IN EVEN-EVEN SELF-CONJUGATE NUCLEI

10th Quantum Phase Transitions in Nuclei and Many-Body Systems

Session 8: clustering and shape phase transitions in nuclei and other systems

Dubrovnik, Croatia | G. STELLIN, K.-H. SPEIDEL and U.-G. MEISSNER

13 July 2022



Introduction

Magnetic Dipole Moments

Theoretical framework

Discretization Effects

Conclusion

Appendix

Motivation: *At decreasing densities, nuclear matter lowers its energy by forming localized α -clusters. The process entails a **quantum phase transition**, driven also by the Pauli principle. The order parameters are the multipolar mass moments, whereas the nuclear density provides the control parameter.*

Phys. Rev. C 102, 014305 (2020)

| We present a novel theoretical interpretation of the **gyromagnetic factors** of light and medium-mass nuclei with even Z and $N = Z, Z + 1, Z + 2$, cf. GS et al. [ArXiv: 2205.10388 \(2022\)](#).

| We investigate rotational symmetry breaking in the magnetic dipole moments of the 2_1^+ and 3_1^- states of ^{12}C induced by the **lattice** configuration space. We, thus, complement the existing literature (e.g. GS et al. [EPJ A 54, 232 \(2018\)](#)) in which in the low-energy states of

light α -conjugate nuclei: ^8Be , ^{12}C , ^{16}O , ...

the dependence of avg. values of *physical observables* on the lattice parameters is explored.

Introduction

Magnetic Dipole Moments

Theoretical framework

Discretization Effects

Conclusion

Appendix

MAGNETIC DIPOLE MOMENTS

Magnetic dipole moment operators serve as a testing ground for

the nuclear A-body wavefunctions | corrections to the free nucleon g-factors and are sensitive to the occupancy of the orbits of the shell-model (SM) quasiparticles

$$= \frac{e}{2m_p} \sum_{i=1}^Z (g_i^p \cdot + g_s^p \mathbf{s}_i) + \frac{e}{2m_n} \sum_{i=1}^N (g_i^n \cdot + g_s^n \mathbf{s}_i),$$

() protons (neutrons)
 ℓ, ℓ angular momentum
 \mathbf{s}, \mathbf{s} spin

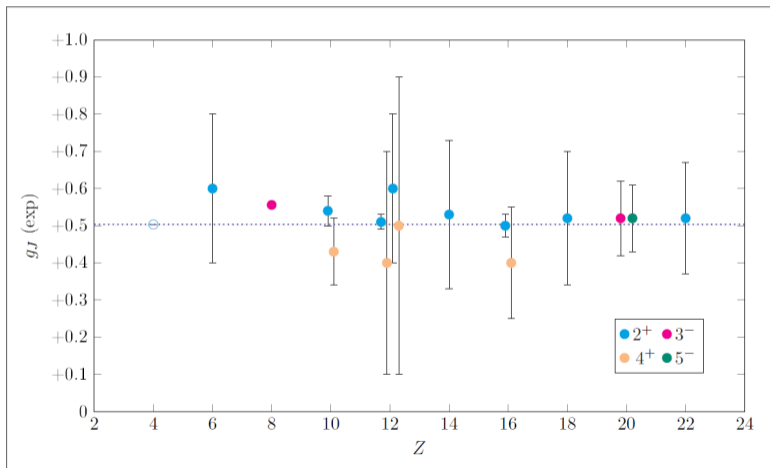
where $g^p = 1$, $g_s^p = 5.5856946893(16)$ and $g^n = 0$, $g_s^n = 3.82608545(90)$ (*free values*).

Remark: In macroscopic α -cluster models for even-even $N=Z$ nuclei $g_s = 0$ and the single α -particle angular momentum operators, ℓ_i sum up to \mathbf{L} , which becomes parallel to :

$$g_L^{(\alpha)} = \frac{e}{2m} \sum_{i=1}^4 g_i \cdot \ell_i = \frac{e g_L^{(\alpha)}}{2m_p} \mathbf{L}$$

$$g_L^{(\alpha)} = g \cdot \frac{m_p}{m} = \frac{2m_p}{m} + 0.5034$$

where m (m_p) denotes the α -particle (proton) mass



Remark:

Almost all the measured g-factor values of the sample of excited 2^+ , 3^- , 4^+ and 5^- states of N=Z 22 nuclei agree with the macroscopic α -cluster prediction of +0.5034 within the statistical errors. The accord remains intact at growing excitation energies.

GYROMAGNETIC FACTORS IN $N=Z$ NUCLEI

Vast literature on α -clustering exists for this category of nuclei. In particular:

NUCLEUS	LEVEL	$g^{(exp)}$	$g^{()}$	$g^{(SM)}$	INTERACTIONS (SM)	REFERENCES (SM)
^8Be	2_1^+		+0.5034			
^{12}C	2_1^+	+0.60(20)	+0.5034	+0.507	Cohen-Kurath	<i>J. Phys. G</i> 8 , 679-685 (1982)
^{16}O	3_1	+0.556(4)	+0.5034	+0.555	Millener-Kurath	<i>J. Phys. G</i> 8 , 679-685 (1982)
^{20}Ne	2_1^+ 4_1^+	+0.54(4) +0.43(9)	+0.5034	+0.510 +0.513	USDB	<i>Phys. Rev. C</i> 96 , 024316 (2017)
^{24}Mg	2_1^+ 4_1^+ 2_2^+ 4_2^+	+0.538(13) +0.40(30) +0.60(20) +0.50(40)	+0.5034	+0.513 +0.518 +0.519 +0.512	USDB	<i>Phys. Rev. C</i> 96 , 024316 (2017)
^{28}Si	2_1^+	+0.53(2)	+0.5034	+0.516	USDB	<i>Phys. Rev. C</i> 96 , 024316 (2017)
^{32}S	2_1^+ 4_1^+	+0.50(3) +0.40(15)	+0.5034	+0.505 +0.507	USDB	<i>Phys. Rev. C</i> 96 , 024316 (2017)
^{36}Ar	2_1^+	+0.52(18)	+0.5034	+0.488	Warburton-Brown	<i>Phys. Lett. B</i> 632 , 207-211 (2016)
^{40}Ca	3_1 5_1	+0.52(10) +0.52(9)	+0.5034	+0.486 +0.512	(RPA)	<i>Phys. Rev. C</i> 10 , 919-922 (1974)
^{44}Ti	2_1^+	+0.52(15)	+0.5034	+0.514	FDP6	<i>Phys. Lett. B</i> 567 , 153-158 (2003)

For a single neutron outside the paired neutron (proton) configuration, the magnetic dipole moment operator reduced approximately to the one of the odd nucleon with $u = \nu$ (π):

$$= \frac{e}{2m_u} (g^u \cdot + g_s^u \mathbf{s})$$

projection along \mathbf{J} :

$$J \frac{e}{2m_u} g_J J = \frac{J (g^u \cdot + g_s^u \mathbf{s})}{J(J+1)^{-2}} \frac{eJ}{2m_u}$$

where $g_J = g^{(SE)}$ coincides with the **Schmidt estimate** of the gyromagnetic factor.

| The inner products are evaluated via the Landé formulae:

$$\langle \mathbf{J} \cdot \mathbf{J} \rangle = \frac{\hbar^2}{2} [J(J+1) + \ell(\ell+1) - s(s+1)] \quad \langle \mathbf{s} \cdot \mathbf{J} \rangle = \frac{\hbar^2}{2} [J(J+1) + s(s+1) - \ell(\ell+1)]$$

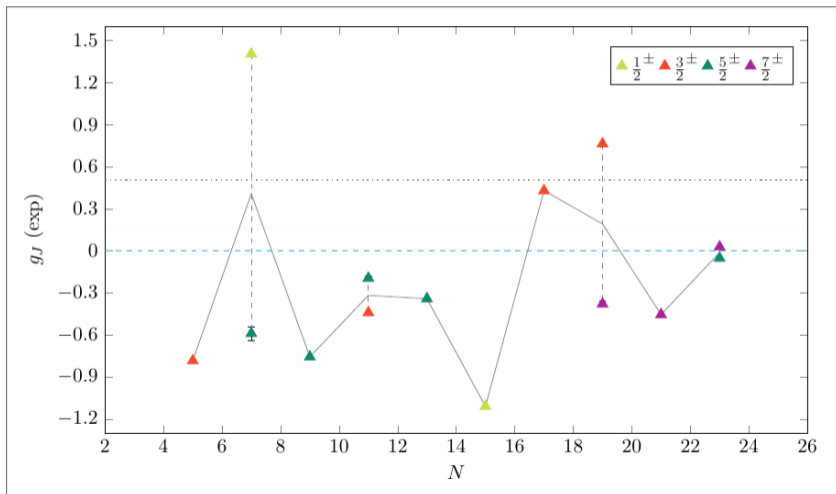
Results: adopting $(g_s^u)^{\text{eff}} = 0.70g_s^u$, the values of $g^{(SE)}$ for the *g.s.* of ${}^9\text{Be}$, ${}^{17}\text{O}$, ${}^{37}\text{Ar}$ and ${}^{41}\text{Ca}$ reproduce quite well the experimental *g*-factors. Still appreciable results are obtained for ${}^{13}\text{C}$ and ${}^{21}\text{Ne}$, whereas moving further away from the shell closures the agreement deteriorates.

GYROMAGNETIC FACTORS IN $N=Z+1$ NUCLEI

$M\alpha + n$ cluster studies exist for ${}^9\text{Be}$ and ${}^{13}\text{C}$ (LCAO, CSM), ${}^{17}\text{O}$ (GCM) and ${}^{21}\text{Ne}$ (CSM).

NUCLEUS	LEVEL	$g^{(exp)}$	$g^{(SE)}$	$g^{(SM)}$	INTERACTIONS (SM)	REFERENCES (SM)
${}^9\text{Be}$	$\frac{3}{2}_1$	-0.784955(2)	-0.89	-0.713	Cohen-Kurath	<i>Nucl. Phys. A</i> 403 , 2, 421-432 (1983)
${}^{13}\text{C}$	$\frac{1}{2}^+$ $\frac{3}{2}^+$ $\frac{5}{2}^+$	+1.404824(2) -0.59(5)	+0.89 -0.77	+1.506 -0.597	Cohen-Kurath	<i>Nucl. Phys. A</i> 403 , 2, 421-432 (1983)
${}^{17}\text{O}$	$\frac{5}{2}^+$	-0.75752(4)	-0.54	-0.7652	USDB	<i>Phys. Rev. C</i> 96 , 024316 (2017)
${}^{21}\text{Ne}$	$\frac{3}{2}^+$ $\frac{5}{2}^+$ $\frac{7}{2}^+$	-0.441198(3) -0.196(12)	0.54	-0.500 -0.230	USDB	<i>Phys. Rev. C</i> 96 , 024316 (2017)
${}^{25}\text{Mg}$	$\frac{5}{2}^+$	-0.34218(3)	-0.54	-0.340	USDB	<i>Phys. Rev. C</i> 96 , 024316 (2017)
${}^{29}\text{Si}$	$\frac{1}{2}^+$	-1.1106(6)	-2.67	-1.114	USDB	<i>Phys. Rev. C</i> 96 , 024316 (2017)
${}^{33}\text{S}$	$\frac{3}{2}^+$ $\frac{5}{2}^+$	+0.4292141(9)	-0.54	+0.387	Chung-Wildenthal	<i>Ann. Rev. Nucl. Part. Sci.</i> 30 , 383-436 (1980)
${}^{37}\text{Ar}$	$\frac{3}{2}^+$ $\frac{7}{2}^+$	+0.763(3) -0.38(2)	+0.54 -0.38	+0.601 -0.43	Glaudemans-Wiechers-Brussaard (Particle-vibration coupling)	<i>Nucl. Phys.</i> 73 , 3, 604-612 (1965) <i>Nucl. Phys. A</i> 251 , 181-192 (1975)
${}^{41}\text{Ca}$	$\frac{7}{2}_1$	-0.455652(3)	-0.38	-0.49	USD, Kuo-Brown and LKS	<i>Phys. Rev. C</i> 91 , 041304(R) (2015)
${}^{45}\text{Ti}$	$\frac{7}{2}_1$ $\frac{5}{2}_1$	+0.027(1) -0.053(4)	-0.38 +0.38	+0.159 -0.292	Kutschera-Brown-Ogawa	<i>Riv. Nuovo Cim.</i> 1 , 2, 1-116 (1978)

GYROMAGNETIC FACTORS IN $N=Z+1$ NUCLEI



Remark:

The experimental g -factor values do not fit the $g^{()}$ (and Z/A) estimates any more. The g_J s are shifted towards negative values, as a result of the spin contribution of the unpaired neutron $g_s^n < 0$.

In excited states, the added neutrons are allowed to lie into two (distinct) single-particle levels. The contribution of each neutron can be evaluated through the Schmidt formula.

the two outcomes can be combined together, giving the overall $g_J = g^{(SE)}$

$$g_J = \frac{g_1 j_1 + g_2 j_2}{J(J+1)^{-2}} \quad J = \frac{1}{2}(g_1 + g_2) + \frac{1}{2} \frac{j_1(j_1 + 1) - j_2(j_2 + 1)}{J(J+1)} (g_1 - g_2) .$$

Results: As expected, the Schmidt estimates turn out to be quite predictive for the semi-magic nuclei of the chain, i.e. ^{14}C , ^{18}O , ^{38}Ar and ^{42}Ca . On the other hand, the g-factors of the open-shell isotopes, are well described by the macroscopic α -cluster value of $+0.5034$.

$g^{(SE)}$ and $g^{(\alpha)}$ provide **complementary** information on the structure of the A-body system

| Shell-closures seem to hinder α -clustering, favouring a more compact spatial distribution of the w.f.

GYROMAGNETIC FACTORS IN $N=Z+2$ NUCLEI

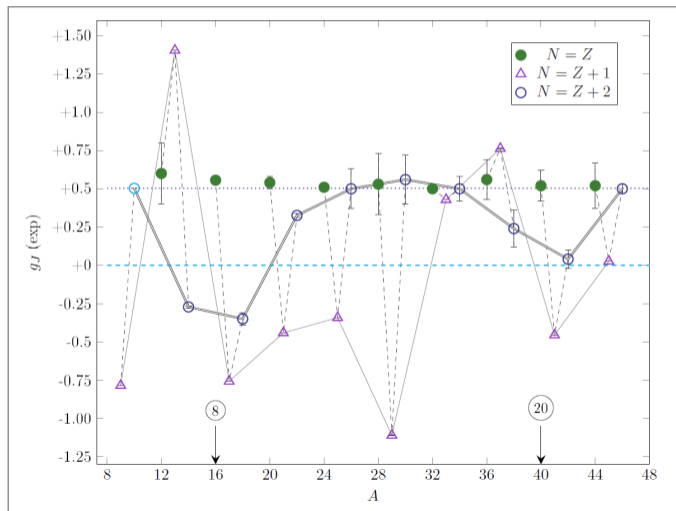
$M\alpha + 2n$ cluster studies exist for ^{10}Be (LCAO) and ^{14}C (AMD+GCM), ^{18}O and ^{22}Ne (GCM).

NUCLEUS	LEVEL	$g^{(exp)}$	$g^{(SE)}$	$g^{(SM)}$	INTERACTIONS (SM)	REFERENCES (SM)
^{10}Be	2_1^+		-0.45	+0.503	χEFT (MCSM)	<i>S. China Mech. and Astr.</i> 57 , 239-243 (2014)
^{10}C	2_1^+		+1.99	+0.802	χEFT (MCSM)	<i>S. China Mech. and Astr.</i> 57 , 239-243 (2014)
^{14}C	3_1	-0.272(7)	-0.30	-0.261	Cohen-Kurath	<i>Phys. Rev. C</i> 9 , 1748 (1974)
^{18}O	3_1	-0.35(4)	-0.20	-0.3995	USDB	<i>Phys. Rev. C</i> 96 , 024316 (2017)
^{22}Ne	2_1^+	+0.326(12)	-0.19	+0.374	USDB	<i>Phys. Rev. C</i> 96 , 024316 (2017)
	4_1^+	+0.55(14)	-0.14	-0.511		
^{26}Mg	2_1^+	+0.50(13)	-0.19	+0.8695	USDB	<i>Phys. Rev. C</i> 96 , 024316 (2017)
^{30}Si	2_1^+	+0.56(16)	-0.27	+0.366	USDB	<i>Phys. Rev. C</i> 96 , 024316 (2017)
^{34}S	2_1^+	+0.50(8)	-0.27	+0.50	Chung-Wildenthal	<i>Mesons in Nuclei II</i> , NH Elsev. (1979)
^{38}Ar	2_1^+	+0.24(12)	-0.84	+0.309	Warburton-Brown	<i>Phys. Rev. C</i> 46 , 923 (1992)
^{42}Ca	2_1^+	+0.04(6)	-0.13	+0.13	USD, Kuo-Brown and LKS	<i>Phys. Lett. B</i> 571 , 1-2, 29-35 (2003)
^{46}Ti	2_1^+	+0.50(3)	-0.13	+0.285	FSM and Kuo-Brown 3	<i>Phys. Rev. C</i> 62 , 024305 (2000)

| **Global plot:** G-factor of the $N = Z$, $Z + 1$ and $Z + 2$ nuclei

Remark:

The measured g-factor values of the excited 2^+ , 3^- and 5^- states of the considered nuclei agree with the macroscopic α -cluster prediction, except for the semi-magic nuclides of the chain. For the latter, **shell-closure** effects prevail, as highlighted by the corresponding Schmidt estimates.



Introduction	Discretization Effects
Magnetic Dipole Moments	Conclusion
Theoretical framework	Appendix

The macroscopic α -cluster model of B. Lu et al. *Phys. Rev. D* **90**, 034507 (2014) is adopted:

$$H = \sum_{i=1}^M \frac{\hbar^2}{2m} k_i^2 + \sum_{i>j=1}^M [V_C(r_{ij}) + V_{AB}(r_{ij})] + \sum_{i>j>k=1}^M V_T(r_{ij}, r_{ik}, r_{jk})$$

with $r_{ij} = \sqrt{r_i^2 + r_j^2}$. The potentials are of the type

Coulomb¹

$$\frac{4e^2}{4} \frac{1}{r_{ij}} \operatorname{erf} \frac{r_{ij}}{R}$$

with $R = 1.44$ fm
rms radius of the ^4He
NB: Erf absorbs the
singularity at $r = 0$

Ali-Bodmer^{1,2}

$$V_0 e^{-\frac{r_{ij}^2}{R_0^2}} + V_1 e^{-\frac{r_{ij}^2}{R_1^2}}$$

with $R_1 = 1.89036$ fm,
 $V_1 = 353.508$ MeV
and $R_0 = 2.29358$ fm,
 $V_0 = 216.346$ MeV,
auxiliary param. $\rho = 1$

Gaussian^{3,4}

$$V_3 e^{-\frac{r_{ij}^2 + r_{ik}^2 + r_{jk}^2}{R^2}}$$

with $R = 0.00506$ fm²,
 $V_3 = 4.41$ MeV for ^{12}C
s.t. $E_{g.s.} = E_{\text{Hoyle}}$
and $V_3 = 10.37(3)$ MeV for ^{16}O
s.t. $E_{g.s.} = E_4$

¹ *Nucl. Phys.* **80**, 99 (1966). , ² *Phys. Rev. C* **70**, 014006 (2004). , ³ *Z. Phys. A* **290**, 93 (1979). , ⁴ G.S. (2020)

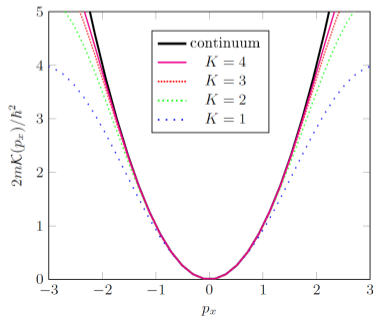
The configuration space in relative d.o.f. of an M -body physical system into a cubic lattice reduces to

$$\mathbb{R}^{3M-3} / \mathbb{N}^{3M-3}$$

where: N number of points per dimension (**lattice size**) and a **lattice spacing** and $L = N a$

Consequences: **discretization effects** ...

1. the action of differential operators is expressed through finite differences
2. breaking of Galilean invariance
3. breaking of continuous translational invariance (free-particle case)



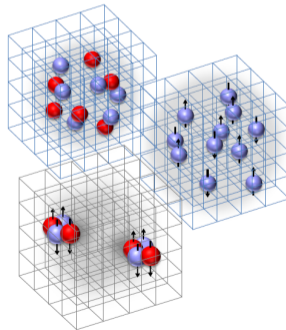
The configuration space in relative d.o.f. of an M body physical system into a cubic lattice reduces to

$$\mathbb{R}^{3M-3} / \mathbb{N}^{3M-3}$$

... and **finite-volume effects**

With periodic boundary conditions:

1. configuration space becomes isomorphic to a torus in $3M-3$ -dimensions
2. lattice momenta become $\mathbf{p} = \sim \frac{2\pi}{Na} \mathbf{n}$ where \mathbf{n} is a vector of integers
3. breaking of $SO(3)$ rotational invariance



On the lattice SO(3) symmetry reduces to the invariance under the **cubic group** O .

Degenerate states belonging to the same irrep of O SO(3, Z) are labeled with the irreps I_z of the cyclic group C_4 , generated by an order-four element of O (e.g. $R_z = e^{i\pi/2}$):

$$\begin{array}{ccc} \text{SO(3)} & & \text{SO(2)} \\ & \& & \\ & j, l, m_i & \end{array}$$

$$\begin{array}{ccc} O & & C_4 \\ & \& & \\ & j, I_z & \end{array}$$

Discrete symmetries are preserved: **time reversal**, **parity**, **exchange symmetry**

Integer spin irreps of SO(3) and SU(2) decompose into irreps of O as follows: $D^0 = A_1$ and

$$\begin{array}{l} D^1 = T_1 \\ D^2 = E \quad T_2 \\ D^3 = A_2 \quad T_1 \quad T_2 \\ D^4 = A_1 \quad E \quad T_1 \quad T_2 \\ D^5 = E \quad T_1 \quad T_1 \quad T_2 \\ D^6 = A_1 \quad A_2 \quad E \quad T_1 \quad T_2 \quad T_2 \end{array}$$

Lattice states (j, N, I_z, S, P) :

N no. of states with the same transf. properties, sorted by their energy in ascending order;

S fully symmetric irrep of the particle permutation group, S_M ;

P parity irrep.

The second quantization formalism is adopted: $a_{iM}^\dagger(\mathbf{n}_{iM})$ ($a_{iM}(\mathbf{n}_{iM})$) creates (annihilates) the α -particle i relative to the α -particle M at the site (\mathbf{n}_{iM}) of the lattice.

Example: the z component of the angular momentum operator

$$(L_{iM})_z = a \sum_{\mathbf{n}_i \in \mathcal{N}} \sum_{k=1}^K \epsilon_{z k} C_k^{(1,K)}(\mathbf{n}_{iM}) \frac{\hbar}{a} a_{iM}^\dagger(\mathbf{n}_{iM} + k\mathbf{e}_z) a_{iM}(\mathbf{n}_{iM}) - a_{iM}^\dagger(\mathbf{n}_{iM} - k\mathbf{e}_z) a_{iM}(\mathbf{n}_{iM})$$

where the coefficients $C_k^{(1,K)} \sim 1/a$ refer to the improvement scheme of the first derivative and K is the total number of hopping terms in the matrix representation of the operator.

The $(L_{iM})_z$ s are the building blocks of the **magnetic dipole moment** operator:

$$\mu(N, \ell, P)^{(r)} = \langle N, \ell, \ell, S, P | j \hat{\mu}_0^{(r)} | N, \ell, \ell, S, P \rangle = \langle N, \ell, \ell, S, P | j \mu_N g_L^{(r)} \sum_{i=1}^N (L_{iM})_z | N, \ell, \ell, S, P \rangle$$

where (r) relative reference frame and $\mu_N = e\hbar/2m_p$.

MULTIPLIET AND ISOTROPIC AVERAGES

With the purpose of reducing the lattice artifacts, one defines two quantities:

Multiplet average *Phys. Rev. D 90, 034507 (2014)*

$$(N, \ell, S, P | Q | N, \ell, S, P)_A \times \frac{X(\ell) X(I_z)}{2\ell + 1} (N, \ell, I_z, S, P | Q | N, \ell, I_z, S, P)$$

where: ℓ $SO(3)$ label of the state in the continuum and infinite-volume limit
 $X_A(a)$ characteristic function, vanishing if the irrep $a \not\supseteq$ decomposition of the irrep A

Isotropic average *Phys. Rev. D 92, 014506 (2015)*

$$(N, \ell, n, S, P | \hat{Q}_q^k | N, \ell, m, S, P) \times \frac{1}{2\ell + 1} \sum_{m^0, m^{00}, m^{000}} (\ell^k \ell^j m q n) (\ell^k \ell^j m^0 m^{00} m^{000}) (N, \ell, m^{000}, S, P | \hat{Q}_{m^0}^k | N, \ell, m^{00}, S, P)$$

where: k rank of the spherical tensor operator $\hat{O}_{m^0}^k$ and $(\ell_1 \ell_2 \ell_3 | m_1 m_2 m_3)$ Clebsch-Gordan coefficient

Introduction	Discretization Effects
Magnetic Dipole Moments	Conclusion
Theoretical framework	Appendix

DISCRETIZATION ON ^{12}C : THE M1 MOMENT OF THE 2^+_1 STATE

| Average value of the magnetic dipole moment of the 2^+_1 state as a function of the lattice spacing. The $(2j^{\wedge}_0j22)$ (open circles) and the *isotropically averaged* counterpart (filled circles) display a local minimum at $a_0^{-1} = 2.29$ fm, in correspondence with a local maximum of the estimate of the M1 moment extracted from the multiplet-averaged value of L^2 (open triangles).

DISCRETIZATION ON ^{12}C : THE M1 MOMENT OF THE 2^+_1 STATE

| Average value of the **magnetic dipole moment** of the 2^+_1 state as a function of the lattice spacing. The theoretical value of $+1.0068 \mu_N$ is marked by a **dotted line**. Deviations of (μ_j / μ_0) from the latter are $\sim 10\%$ in the $a \in [1.5, 1.75]$ fm region. FV effects are suppressed by the constraint $Na \leq 19$ fm.

DISCRETIZATION ON ^{12}C : THE M1 MOMENT OF THE 2^+_1 STATE

| Reduced matrix elements contributing to the **isotropic average** (**solid line with full circles**) of the M1 moment of the 2^+_1 state as a function of the lattice spacing. The latter correspond to matrix elements of the *spherical component* of \hat{m}_m between the states $|2m^0\rangle$ and $|2m^{00}\rangle$, divided by the Clebsch-Gordan coefficient $(212jmm^0m^{00})$.

DISCRETIZATION ON ^{12}C : THE M1 MOMENT OF THE 2^+_1 STATE

| Reduced matrix elements contributing to the **isotropic average** (**solid line with full circles**) of the M1 moment of the 2^+_1 state as a function of the lattice spacing. The asymptotic value of the *reduced* matrix elements (**dotted line**) is equal to $\sqrt{\frac{2}{3}} \frac{m_p}{m} = 1.2331$.

DISCRETIZATION ON ^{12}C : THE M1 MOMENT OF THE 3_1 STATE

| Average value of the **magnetic dipole moment** of the 3_1 state as a function of the lattice spacing. The $(3j^0_0/33)$ (**open circles**) and the *isotropically averaged* counterpart (**filled circles**) display a local minimum at $a_0^{-1} = 2.29$ fm, in correspondence with a local maximum of the estimate of the M1 moment extracted from the multiplet-averaged value of L^2 (**open triangles**).

DISCRETIZATION ON ^{12}C : THE M1 MOMENT OF THE 3_1 STATE

| Average value of the **magnetic dipole moment** of the 3_1 state as a function of the lattice spacing. The theoretical value of $+1.5102 \mu_N$ is marked by a **dotted line**. Deviations of (μ_j^0/μ_j) from the latter are 10% in the $a \in [1.75, 1.9]$ fm region. FV effects are suppressed by the constraint $Na \leq 19$ fm.

DISCRETIZATION ON ^{12}C : THE M1 MOMENT OF THE 3_1 STATE

I Reduced matrix elements contributing to the **isotropic average** (solid line with full circles) of the M1 moment of the 3_1 state as a function of the lattice spacing. The latter correspond to matrix elements of the *spherical component* of \hat{m}_m between the states $|3m^0\rangle$ and $|3m^{00}j\rangle$, divided by the Clebsch-Gordan coefficient $(313jmm^0m^{00})$.

DISCRETIZATION ON ^{12}C : THE M1 MOMENT OF THE 3_1 STATE

| Reduced matrix elements contributing to the isotropic average (solid line with full circles) of the M1 moment of the 3_1 state as a function of the lattice spacing. The asymptotic value of the *reduced* matrix elements (dotted line) is equal to $+2\sqrt{\frac{2}{3}} \frac{2m_p}{m} = 1.7438$. The isotropic average brings significant suppression of the discr. artifacts in the $a < 3.0$ fm region.

Introduction

Magnetic Dipole Moments

Theoretical framework

Discretization Effects

Conclusion

Appendix

- | The literature on M1 moments has been complemented by paralleling the average values of the magnetic dipole operator for α -conjugate nuclei from ^{12}C to ^{44}Ti with the partitioning of nuclear matter into ^4He clusters. For nuclei with even Z , it has been shown that the exp. g -factors of excited states of $N=Z$ nuclei assume the same value, $g = +0.50$;

- | The literature on M1 moments has been complemented by paralleling the average values of the magnetic dipole operator for α -conjugate nuclei from ^{12}C to ^{44}Ti with the partitioning of nuclear matter into ^4He clusters. For nuclei with even Z , it has been shown that
 - the exp. g -factors of excited states of $N=Z$ nuclei assume the same value, $g = +0.50$;
 - for semi-magic nuclei the appended two neutrons determine the g -factors;

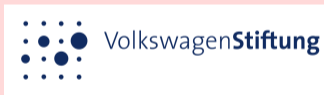
- | The literature on M1 moments has been complemented by paralleling the average values of the magnetic dipole operator for α -conjugate nuclei from ^{12}C to ^{44}Ti with the partitioning of nuclear matter into ^4He clusters. For nuclei with even Z , it has been shown that
 - the exp. g-factors of excited states of $N=Z$ nuclei assume the same value, $g = +0.50$;
 - for semi-magic nuclei the appended two neutrons determine the g-factors;
 - outside the shell closures, for $N = Z + 2$ nuclei the added neutrons lose their influence and the macroscopic α -cluster predictions are aligned with the exp. g-factors.

- | The literature on M1 moments has been complemented by paralleling the average values of the magnetic dipole operator for α -conjugate nuclei from ^{12}C to ^{44}Ti with the partitioning of nuclear matter into ^4He clusters. For nuclei with even Z , it has been shown that
 - the exp. g-factors of excited states of $N=Z$ nuclei assume the same value, $g = +0.50$;
 - for semi-magic nuclei the appended two neutrons determine the g-factors;
 - outside the shell closures, for $N = Z + 2$ nuclei the added neutrons lose their influence and the macroscopic α -cluster predictions are aligned with the exp. g-factors.
- | The macroscopic lattice model in [EPJ A 54, 232 \(2018\)](#) for light α -conjugate nuclei has been recapitulated. A parallel implementation of Lanczos iteration on GPUs was adopted for the diagonalization of the Hamiltonian, allowing for

- | The literature on M1 moments has been complemented by paralleling the average values of the magnetic dipole operator for α -conjugate nuclei from ^{12}C to ^{44}Ti with the partitioning of nuclear matter into ^4He clusters. For nuclei with even Z , it has been shown that
 - the exp. g-factors of excited states of $N=Z$ nuclei assume the same value, $g = +0.50$;
 - for semi-magic nuclei the appended two neutrons determine the g-factors;
 - outside the shell closures, for $N = Z + 2$ nuclei the added neutrons lose their influence and the macroscopic α -cluster predictions are aligned with the exp. g-factors.
- | The macroscopic lattice model in [EPJ A 54, 232 \(2018\)](#) for light α -conjugate nuclei has been recapitulated. A parallel implementation of Lanczos iteration on GPUs was adopted for the diagonalization of the Hamiltonian, allowing for
 - the study of discretization effects in the the M1 moment of the 2_1^+ and 3_1^- states of ^{12}C , with the computation of the isotropic averages (cf. [Phys. Rev. D 92, 014506 \(2015\)](#)).

- | The literature on M1 moments has been complemented by paralleling the average values of the magnetic dipole operator for α -conjugate nuclei from ^{12}C to ^{44}Ti with the partitioning of nuclear matter into ^4He clusters. For nuclei with even Z , it has been shown that
 - the exp. g -factors of excited states of $N=Z$ nuclei assume the same value, $g = +0.50$;
 - for semi-magic nuclei the appended two neutrons determine the g -factors;
 - outside the shell closures, for $N = Z + 2$ nuclei the added neutrons lose their influence and the macroscopic α -cluster predictions are aligned with the exp. g -factors.
 - | The macroscopic lattice model in [EPJ A 54, 232 \(2018\)](#) for light α -conjugate nuclei has been recapitulated. A parallel implementation of Lanczos iteration on GPUs was adopted for the diagonalization of the Hamiltonian, allowing for
 - the study of discretization effects in the the M1 moment of the 2_1^+ and 3_1^- states of ^{12}C , with the computation of the isotropic averages (cf. [Phys. Rev. D 92, 014506 \(2015\)](#)).
- Outlook** (in progress): Calculation of the magnetic dipole moments of low-lying excited states of even-even $N = Z, Z + 2$ nuclei from the Lehmann's representation of the polarization propagator in the ab-initio **self-consistent Gorkov-Green's function approach** (SCGGF).

Financial resources



Computational resources



Hvala na pažnji.
Thank you for the attention.

Commissariat à l'énergie atomique et aux énergies alternatives
Etablissement de Saclay | 91 191 Gif-sur-Yvette Cedex
T. (siège) +33 (0)1 69 08 60 00 | T. (bureau) +33 (0)1 69 08 75 75

DPhN
Irfu
SPhN

Établissement public à caractère industriel et commercial | RCS Paris B 775 685 019

Introduction

Magnetic Dipole Moments

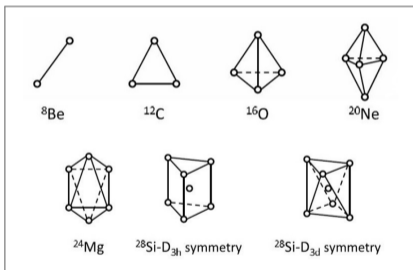
Theoretical framework

Discretization Effects

Conclusion

Appendix

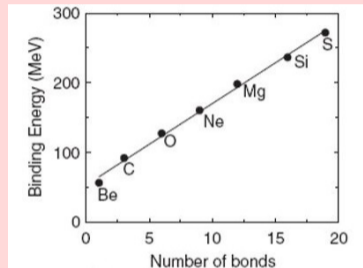
The idea to group the nucleons into ${}^4\text{He}$ clusters has been advanced at the dawn of nuclear physics.



J.A. Wheeler, *Phys. Rev.* **52**, 1083 (1937)

W. Wefelmaier, *Zeitschr. für Phys.* **107**, 332 (1937)

D. M. Dennison, *Phys. Rev.* **57**, 454 (1940)



Linear behaviour of $BE(Z, N)$ as a function of the number of bonds between the ${}^4\text{He}$ -clusters at the vertices of ordered structures L.R. Hafstad and E. Teller, *Phys. Rev.* **54**, 681 (1938)

Comprehensive review on α -clustering:

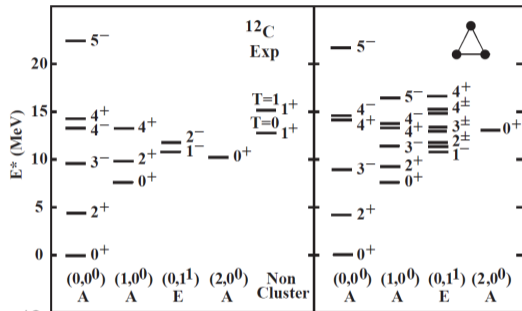
cf. M. Freer et al., *Rev. Mod. Phys.* **90**, 035004 (2018)

Macroscopic models

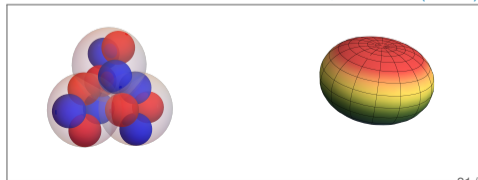
The **proton** and **neutron** degrees of freedom are suppressed in favour of α particles, stable bosons of zero total spin and isospin

- | with phenomenological potentials: S. Ali & A.R. Bodmer, O. Portilho, S.I. Fedotov, ...
- | obeying symmetry principles:

- | **normal modes of vibration** & rotations for ^{12}C (D_{3h}): *J. of Phys. G.* **43**, 8 (2016)
- for ^{20}Ne (D_{3h}): *N. P. A* **1006**, 122077 (2021)
- | the **Algebraic Cluster Model** the spectrum of ^{12}C (D_{3h}), ^{16}O (T_d), ... from geometrical principles



- | ^{12}C as an **oblate** rotor: *PRL* **113**, 012502 (2014)



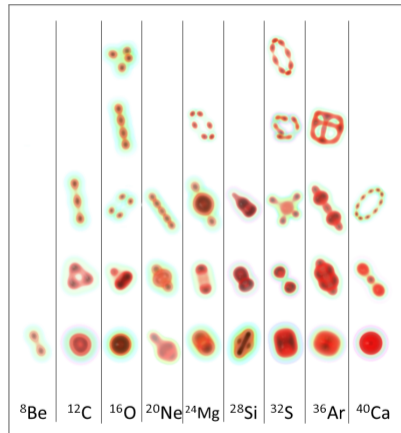
Microscopic models

Single-nucleon degrees of freedom are retained

- | RGM (J.A. Wheeler), GCM (D.M. Brink), OCM ...

Heavier α -conjugate nuclei have been investigated via
Density Functional Theory: J.P. Ebran, E. Khan, ...

- | **Nuclear Lattice Effective Field Theory**: D. Lee, U.-G. Meißner, T.A. Lähde, E. Epelbaum, S. Shen, ...



N *Phys Rev C* **90**, 054329 (2014)

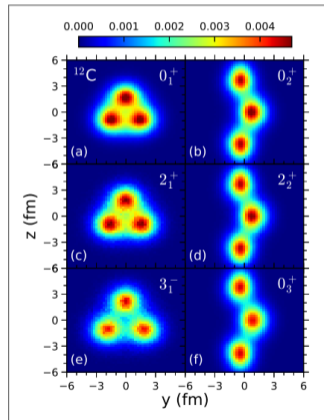
N *PRL* **109**, 252501 (2012)

N *PRL* **112**, 102501 (2014)

Microscopic models

Single-nucleon degrees of freedom are retained in the Hamilt.

- | RGM (J.A. Wheeler), GCM (D.M. Brink), OCM (Saito), ...
- Heavier α -conjugate nuclei have been investigated via **Density Functional Theory**: J.P. Ebran, E. Khan, T. Nikšić, ...
- | **Nuclear Lattice Effective Field Theory**: D. Lee, U.-G. Meißner, T.A. Lähde, S. Elhatisari, S. Shen, H. Krebs, ...



N [ArXiv: 2202.13596 \(2022\)](https://arxiv.org/abs/2202.13596)

N [PRL 109, 252501 \(2012\)](https://doi.org/10.1126/science.1220511)

N [PRL 112, 102501 \(2014\)](https://doi.org/10.1126/science.1250511)

A unitary transformation maps states with given ℓ and m onto states with defined ℓ and I_z :

$$|j\ell, m, I_z\rangle = \sum_{m^0} \chi(g) D_{m^0 m}^j(g) |j\ell, m^0\rangle$$

where $I_z = \text{mod}(m, 4)$ and $\chi(g)$ denotes the *character* of the element $g \in O$ with respect to the irrep and $D_{m^0 m}^j(g)$ is a *Wigner D-matrix*. **Convention:** $|j\ell, m, 1\rangle = |j\ell, m, 3\rangle$

	ℓ	0
	$I_z m$	0
A_1	0	1
	ℓ	1
	$I_z m$	1 0 1
T_1	0	1
	1	1
	3	1

	ℓ	2	1	0	1	2
	$I_z m$	2	1	0	1	2
E	0			1		
	2	$i^{p_{1/2}}$				$i^{p_{1/2}}$
T_2	1				1	
	2	$i^{p_{1/2}}$				$i^{p_{1/2}}$
	3		1			

	ℓ	3	2	1	0	1	2	3
	$I_z m$	3	2	1	0	1	2	3
A_2	2		$i^{p_{1/2}}$				$-i^{p_{1/2}}$	
T_1	0				1			
	1	$i^{p_{1/2}}$				$i^{p_{1/2}}$		
	3		$i^{p_{1/2}}$					$i^{p_{1/2}}$
T_2	1	$i^{p_{1/2}}$				$i^{p_{1/2}}$		
	2		$i^{p_{1/2}}$				$i^{p_{1/2}}$	
	3			$i^{p_{1/2}}$				$i^{p_{1/2}}$

DIAGONALIZATION OF THE LATTICE HAMILTONIAN

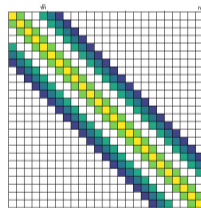
Due to extent of the lattice configuration space, the usage of memory-saving techniques for the diagonalization of the Hamiltonian becomes mandatory.

for ^{12}C @ $N = 32$: an **eigenvector** has $1.073 \cdot 10^9$ entries !

| **Lanczos method**: *the exact eigenvector is extracted by repeated application of the matrix to a trial state with a nonzero component in the direction of the former.*

The process returns the *lowest* signed eigenvector of the Hamiltonian [Nucl. Phys. A 768, 3-4, 179-193 \(2006\)](#).

| By means of the projectors over the irreps of the discrete symmetry groups of the Hamiltonian, O , C_4 , P , S_M, \dots applied at each step of the iterative process the entire spectrum of the matrix can be explored.



Band diagonal structure of the Hamiltonian matrix N

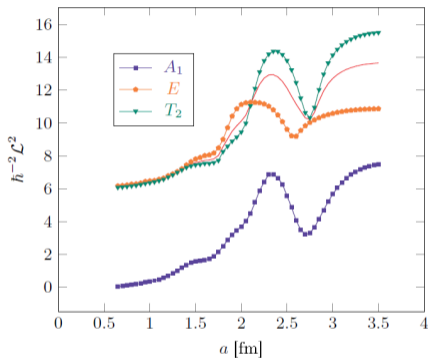
Caveat: due to the increase in the iteration time with N , the usage of graphic cards (GPUs) on side of the CPUs is recommendable, otherwise the calculations $N \approx 20$ for ^{12}C become impractical.

- | Energy eigenvalues of the 2_E^+ (pentagons), $2_{T_2}^+$ (triangles) and $0_{A_1}^+$ (squares) states as a function of the lattice spacing.
- | Spatial distribution of the PDF of the 2_E^+ state with $I_z = 0$ in the slice with $r_{23} = a(5, 1, 0)$ and $a = 0.65$ fm of the configuration space.

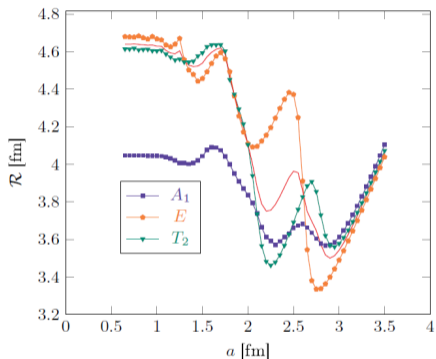
DISCRETIZATION ON ^{12}C : THE ENERGY OF THE 0_1^+ AND 2_1^+ STATES

- For the 2_E^+ ($2_{T_2}^+$) states, the E_r minima lie at 1.50 (1.40), 2.35 (2.40) and 3.20 (3.22) fm. Residual FV errors $\approx 5 \cdot 10^{-3}$ MeV.
- The *isohypsic* correspond to a probability density of 10% its maximum value, found at the bulges of the 'torus' (principal maxima) at $r_{13} = 3.3$ fm.

DISCRETIZATION ON ^{12}C : THE 0_1^+ AND 2_1^+ STATES



Average value of the squared angular momentum for the $0_{A_1}^+$, 2_E^+ and $2_{T_2}^+$ states. In the region $a > 1.25$ fm the exact eigenvalues are reached approximately as $\exp(mj - L^2/j)$ with $m < 0$.



Average value of the separation for the $0_{A_1}^+$, 2_E^+ and $2_{T_2}^+$ states. Residual FV effects for the 2_1^+ multiplets amount to $\approx 10^{-1}$ fm.

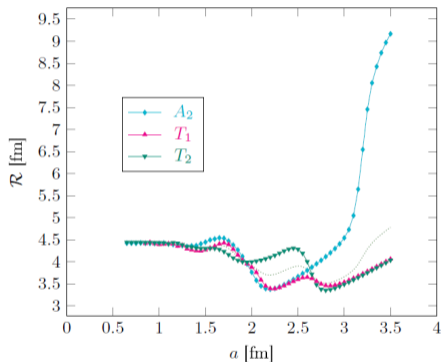
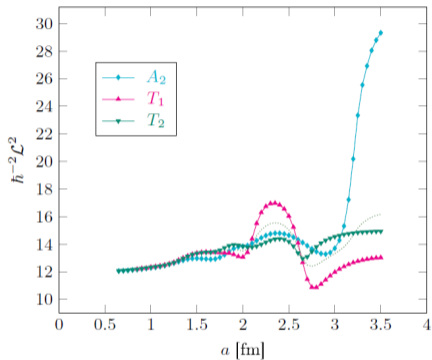
DISCRETIZATION ON ^{12}C : THE ENERGY OF THE 3_1 STATE

- | Energy eigenvalues of the 3_{A_2} (diamonds), 3_{T_2} (up triangles) and 3_{T_1} (down squares) states as a function of the lattice spacing.
- | Spatial distribution of the PDF of the 3_{T_1} state with $l_z = 0$ in the slice with $r_{23} = a(1, 2, 5)$ and $a = 0.65$ fm of the configuration space.

DISCRETIZATION ON ^{12}C : THE ENERGY OF THE 3_1 STATE

- | For the 3_{T_1} (3_{T_2}) states, the E_r minima lie at 1.40 (=), 2.30 (2.35) and 3.18 (=) fm. Residual FV errors $5 \cdot 10^{-3}$ MeV.
- | The *isohypsic* correspond to a probability density of 10% its maximum value, found at the bulges of the 'torus' (principal maxima) at $r_{13} = 3.3$ fm.

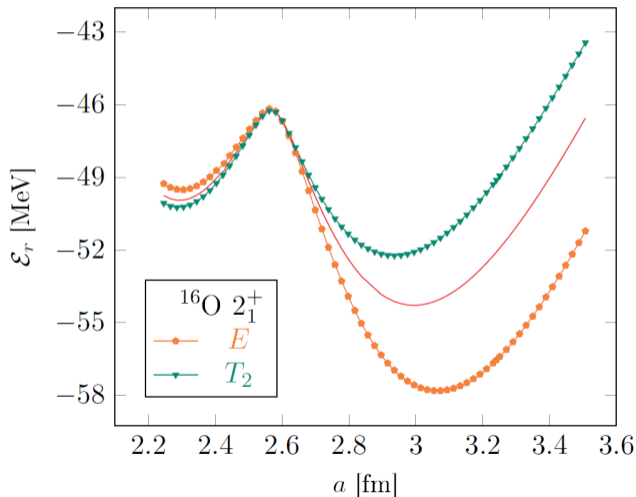
DISCRETIZATION ON ^{12}C : THE 3_1 STATE



Average value of the squared angular momentum for the 3_{A_2} , 3_{T_1} and 3_{T_2} states. In the region $a \lesssim 1.25$ fm the exact eigenvalues are reached as $\exp(mj \cdot L^2 j)$ with $m < 0$.

Average value of the separation for the 3_{A_2} , 3_{T_1} and 3_{T_2} states. Residual FV effects for the 3_1 multiplets amount to $\sim 10^{-1}$ fm.

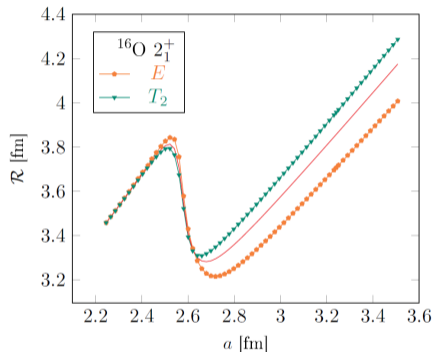
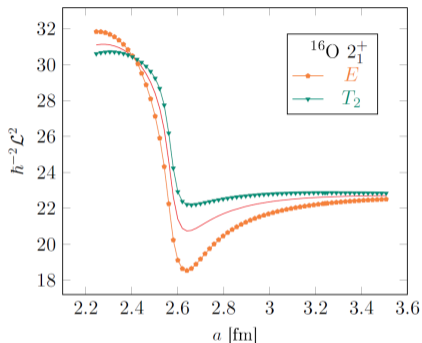
DISCRETIZATION ON ^{16}O : THE ENERGY OF THE 2_1^+ STATE



| **Energy** eigenvalue of the first 2_1^+ and 2_2^+ states as a function of the lattice spacing. The strength parameter, V_3 , of the 3-body potential has been set to 10.33 MeV. Since the 0_1^+ state is fitted to -14.43 MeV, the energy of the experimental 2_1^+ state becomes 7.51 MeV.

| **Remark:** Although at $a = 2.24$ fm discretization effects are large, $\hbar E_r(2_1^+) - E_r(0_1^+) = 6.93$ MeV, in surprising agreement with the experimental counterpart 6.92 MeV. Residual FV errors are suppressed by the constraint $Na = 20$ fm.

DISCRETIZATION ON ^{16}O : THE 2_1^+ STATE



| Average value of the **squared angular momentum** for the 2_E^+ and $2_{T_2}^+$ states. As for ^{12}C , a maximum is detected in at $a_0^1 = 2.29$ fm, where the deviation from the exact eigenvalue amounts to $\sim 25^{-2}$.

| Average value of the **separation** for the 2_E^+ and $2_{T_2}^+$ states. Residual finite-volume errors are suppressed by the constraint $Na \geq 20$ fm.